V European Conference on Computational Fluid Dynamics
ECCOMAS CFD 2010
J. C. F. Pereira and A. Sequeira (Eds)
Lisbon, Portugal, 14–17 June 2010

NUMERICAL SIMULATION OF ROD STABILIZED FLAMES

B. Manickam[*], S. P. R. Muppala[†], J. Franke[††], and F. Dinkelacker[*]

[*] Institute of Technical Combustion, Leibniz University of Hannover
Welfengarten 1a, 30167 Hannover, Germany
e-mail: manickam@itv.uni-hannover.de
e-mail: dinkelacker@itv.uni-hannover.de

[†]Faculty of Engineering, Kingston University
Friars Avenue, Roehampton Vale, London, SW15 3DW, United Kingdom
e-mail: s.muppala@kingston.ac.uk

[††]Institute of Fluid- and Thermodynamics, University of Siegen
Paul-Bonatz-Straße 9-11, 57076 Siegen, Germany
e-mail: franke@ift.mb.uni-siegen.de

Keywords: Combustion Modelling, Numerical Simulation, Rod stabilized flame, Drag Force

Abstract. *An Algebraic Flame Surface Wrinkling model developed and tested for a variety of flame configurations under various flow conditions is used for validation studies of rod-stabilized flames measured by Pfadler et al., LTT Erlangen, Germany. For this methane and propane-air mixtures for equivalence ratios 0.8 and 0.87 at mass flow rates of 9 and 25 kg/hr at atmospheric pressure, respectively, are used. The flame stabilizes due to recirculation region formed behind the rod. Non-reacting flow simulations are carried out with RNG k-ε and LES Smagorinsky subgrid scale model. One of the important differences between the two model predictions is that the k-ε model predicts no vortex shedding, while at the same conditions LES shows vortex shedding frequency of 110 & 360 Hz (and Strouhal numbers 0.154 & 0.18) for 9 and 25 kg/hr respectively. Mean flow quantities from both models are generally in good agreement with experiments. For reacting flows, k-ε predictions are in comparison with experimental half flame angle. These results are also compared with predictions from a popular turbulent flame closure model. The drag force analysis reveals that the drag coefficient (C_d) increases for the reacting flows by 10-50 % as compared to C_d of non reacting flows. We found that C_d shows significant deviation due to inlet flow rate, while it is less sensitive to fuel type and fuel composition. Interestingly, LES appears to show slightly different trends: the drag force coefficient decreases for reacting flow. More LES and further analysis are being carried out to study the role of flame anchoring position on C_d.*

1 INTRODUCTION

Premixed turbulent combustion is of paramount industrial importance as it offers low emissions and high thermal efficiencies. However, it remains a significant research challenge in terms of modelling and simulation of combustion under lean conditions. Modelling and simulation of such combustion processes are complicated due to the interaction between chemical reaction and turbulence. Several combustion models were developed and validated for different experimental configurations. The Algebraic Flame Surface Wrinkling (AFSW) model based on the progress variable approach developed and validated, namely, for Bunsen-like flames and a sudden expansion dump combustor [1] is used. Rod stabilized V-flame is one of the well known labour experiments to analyse the flame instabilities and for validation of the reaction models.

Although a number of V-flame RANS computations were carried out in 2D domain, only few such studies are performed in 3D domain, namely, DNS [2]. In the present study, both RANS and LES approaches are used to investigate a rod stabilized premixed V-flame. It is noted here that V-flame (or cylindrical rod-stabilized flame) instabilities are of fundamental importance since this configuration is frequently used to test the basic mechanism occurring in more practical devices. Flow past the cylinder [3] is also of great interest, due to different effects such as boundary layer separation and wake flow, vortex shedding and resulting lift and drag forces. Many studies have been carried out in this direction to analyze the effects of these flow phenomena as a function of flow Reynolds number. There are some results published by varying cylinder temperature [4], length to diameter ratio [3] etc. In this study, we simulate non-reacting and reacting flows over a cylindrical rod of 1.6 mm diameter; also the drag force is analyzed in terms of drag coefficient at the same conditions.

The remainder of the paper is organized as follows. Following is a brief description of the numerical details is discussed. In the subsequent section, the problem is discussed with geometry and considered boundary conditions for simulations. In the later part, non-reacting and reacting flow results for two different mass flow rates and two (AFSW and turbulent flame speed closure) combustion models are presented and discussed. Finally conclusions are drawn in the final section.

2 NUMERICAL DETAILS – TURBULENCE AND REACTION MODELS

2.1 The RNG κ–ε model

The current is carried out in both reacting and non reacting conditions, since reacting is connected with large density variation; a density weighted averaging procedure is suitable for all the flow and combustion quantities,

$$\tilde{u} = \frac{\overline{\rho u}}{\overline{\rho}}$$

Favre averaged continuty and momentum equations involving turbulent stresses which are modelled as follows

$$\frac{\partial \overline{\rho}}{\partial t} + \frac{\partial}{\partial x_i}(\overline{\rho}\tilde{u}_i) = 0$$

$$\frac{\partial \tilde{u}_i}{\partial t}+\frac{\partial}{\partial x_i}(\tilde{u}_i\tilde{u}_j)=-\frac{1}{\rho}\frac{\partial \overline{p}}{\partial x_j}+\frac{\partial}{\partial x_i}\left[\nu\frac{\partial \tilde{u}_i}{\partial x_i}-\nu_t\left(\frac{\partial \tilde{u}_i}{\partial x_i}+\frac{\partial \tilde{u}_i}{\partial x_i}\right)-\frac{2}{3}k\delta_{ij}\right]$$

where, ν_t is the turbulent eddy viscosity, calcuated using the following relation.

$$\nu_t = C_\mu \frac{k^2}{\varepsilon}$$

where, C_μ = 0.0845, k and ε are the turbulent kinetic energy and dissipation rate of turbulence. Two addition transport equations are solved for prediction of k and ε and the corresponing transport equations are as follows,

$$\left(\frac{\partial k}{\partial t}+\tilde{u}_i\frac{\partial k}{\partial x_i}\right)=\nu_t S^2+\frac{\partial}{\partial x_i}\left(\sigma_k\nu_t\frac{\partial k}{\partial x_j}\right)-\varepsilon$$

$$\frac{\partial \varepsilon}{\partial t}+\tilde{u}_i\frac{\partial \varepsilon}{\partial x_i}=C_{\varepsilon 1}\frac{\varepsilon}{k}\nu_t S^2+\frac{\partial}{\partial x_i}\left(\sigma_\varepsilon\nu_t\frac{\partial \varepsilon}{\partial x_i}\right)-C_{\varepsilon 2}\frac{\varepsilon}{k}-R$$

Where,

$$S=\sqrt{2S_{ij}S_{ij}}\quad ;\ S_{ij}=\frac{1}{2}\left(\frac{\partial u_i}{\partial x_j}+\frac{\partial u_j}{\partial x_i}\right);C_{\varepsilon 1}=1.42,C_{\varepsilon 2}=1.68,\sigma_k=1.39$$

2.2 Large eddy simulation

In the LES approach, the time-dependent three-dimensional continuity and Navier-Stokes equations describing the flow field are given in their filtered form. As an illustration, a filtered variable is defined as

$$\tilde{\phi}(x)=\frac{1}{V}\int\phi(x')G_\Delta(x,x')dx'$$

$$G_\Delta(x,x')=\begin{cases}1/V\\0\end{cases}$$

The filtering process effectively filters out eddies whose scales are smaller than the filter width, which is equal to the local cell volume of the numerical grids in the present computations.

Favre filtering [5-7] of the continuity and momentum equations results in

$$\frac{\partial \overline{\rho}}{\partial t}+\frac{\partial}{\partial x_i}(\overline{\rho}\tilde{u}_i)=0$$

$$\frac{\partial \overline{\rho}\tilde{u}_i}{\partial t}+\frac{\partial}{\partial x_i}(\overline{\rho}\tilde{u}_i\tilde{u}_j)=-\frac{\partial \overline{p}}{\partial x_j}+\frac{\partial}{\partial x_i}\left[\tau_{ij}^{mol}-\tau_{ij}^{sub}\right]$$

$$\tau_{ij}^{sub}=\overline{\rho}(\widetilde{u_iu_j}-\tilde{u}_i\tilde{u}_j)$$

The resulting equations govern the dynamics of the large eddies. These equations are solved with a three-dimensional finite volume CFD code [8]. The Smagorinsky model is the oldest subgrid scale model and still very popular because of its simple formulation.

Unresolved subgrid scale momentum fluxes are expressed according to the Boussinesq assumption [5, 6]

$$\tau_{ij} - \frac{\delta_{ij}}{3}\tau_{kk} = -\nu_t\left(\frac{\partial \tilde{u}_i}{\partial x_j} + \frac{\partial \tilde{u}_j}{\partial x_i}\right) = -2\nu_{sgs}\tilde{S}_{ij}$$

where ν_{sgs} is the subgrid scale viscosity,

$$\nu_{sgs} = C_s^2 \Delta^{4/3} l_{sgs}^{2/3} \left|\tilde{S}\right|$$

Here l_{sgs} is the turbulent integral length scale and C_s a model constant. Using $l_{sgs} = \Delta$ the Smagorinsky model is obtained.

$$\nu_{sgs} = (C_s \Delta)^2 \left|\tilde{S}\right|$$

2.3 Reaction model for premixed turbulent combustion

A well-known approach to describe turbulent premixed combustion is in terms of a scalar variable *c*, instead of the actual chemical species and temperature. The variable *c*, also called reaction progress variable, generalizes reacting species and describes the combustion, which is '0' in reactants and '1' in products. It is defined as

$$c = \frac{T - T_u}{T_a - T_u}$$

where T_u and T_a are the unburned mixture and adiabatic flame temperature, respectively. The transport equation for the Favre filtered progress variable $\tilde{c}$, with gradient diffusion model for the subgrid scale scalar flux, is expressed as

$$\frac{\partial}{\partial t}(\bar{\rho}\tilde{c}) + \frac{\partial}{\partial x_k}(\bar{\rho}\widetilde{u_k c}) = \frac{\partial}{\partial x_k}\left(\bar{\rho}\left(\frac{\nu_{sgs}}{Sc_{sgs}} + \nu\right)\frac{\partial \tilde{c}}{\partial x_k}\right) + \overline{\dot{w}}_c$$

where $\bar{\rho}$ is the mean gas density, ν is the molecular kinematic viscosities, Sc_{sgs}(= 0.7) is the subgrid scale Schmidt number and $\overline{\dot{w}}_c$ is the mean reaction source term, $\overline{\dot{w}}_c = \rho_u S_{L0} I_0 \Sigma$. Here s_{L0} is the unstretched laminar burning velocity, I_0 (=1) the flame stretch factor and Σ the average flame surface density [6].

A RANS-based AFSW model in which Σ is modeled with an algebraic relation for the flame-surface-wrinkling factor $A_T / \overline{A}$, with embedded pressure effects, is used [1].

$$\frac{A_T}{\overline{A}} = \frac{S_T}{S_{L0}} = 1 + \frac{0.46}{e^{(Le-1)}} Re_t^{0.25} \left(\frac{u'}{S_{L0}}\right)^{0.3} \left(\frac{p}{p_0}\right)^{0.2}$$

The RANS model is reformulated with subgrid scale quantities for LES. The relation between RANS and LES models has been analysed by Pitsch et al. [9]. For turbulent flame speed closures he stated that it is possible to extend the reaction model from RANS to LES by replacing the turbulent quantities by subgrid scale quantities. The Favre filtered subgrid scale reaction variable is then divided into two parts, the large

scale resolved flame and the subgrid flame modeled with subgrid flow quantities. For LES the AFSW reaction model is therefore as follows

$$\bar{\dot{w}}_c = \rho_u S_{L0} \frac{A_T^{\Delta}}{\bar{A}} \cdot \left|\nabla \tilde{c}\right|$$

$$\frac{A_T^{\Delta}}{\bar{A}} = \frac{S_T^{\Delta}}{S_{L0}} = 1 + \frac{0.46}{e^{(Le-1)}} Re_{sgs}^{\Delta\ 0.25} \left(\frac{u'_{sgs}}{S_{L0}}\right)^{0.3} \left(\frac{p}{p_0}\right)^{0.2}$$

Le - The Lewis number of the fuel-air mixture

p/p_0 - normalized operating pressure

u'_{sgs} - subgrid turbulence fluctuation $u'_{sgs} = c_S \Delta \left|\tilde{S}\right|$,

Re_{sgs}^{Δ} - subgrid Reynolds number $Re_{sgs}^{\Delta} = u'_{sgs} c_s \Delta / \nu$

In addition to the AFSW model, the Turbulent Flame speed Closure (TFC) of Zimont [10] is used in RANS context and the further details can be found in [10].

3 NUMERICAL GEOMETRY AND BOUNDARY CONDITIONS

Pfadler et al. [11] carried out experiments with rod stabilished flame at atmoshperic pressure and the experimental setup is shown the Fig. 1. Fuel-air mixture was supplied in the center pipe surrounded by coflow of air was supplied in order to avoid the external distances to the flame. A rod of 1.6 mm diameter is fixed in the holder 10 mm above the exit of the inlet pipe. This creates a recirculation region which stabilishes the flame for reaction flow conditions. PIV measurement technique with 1.0 mm TiO_2 partcles as tracer was used for measurements.

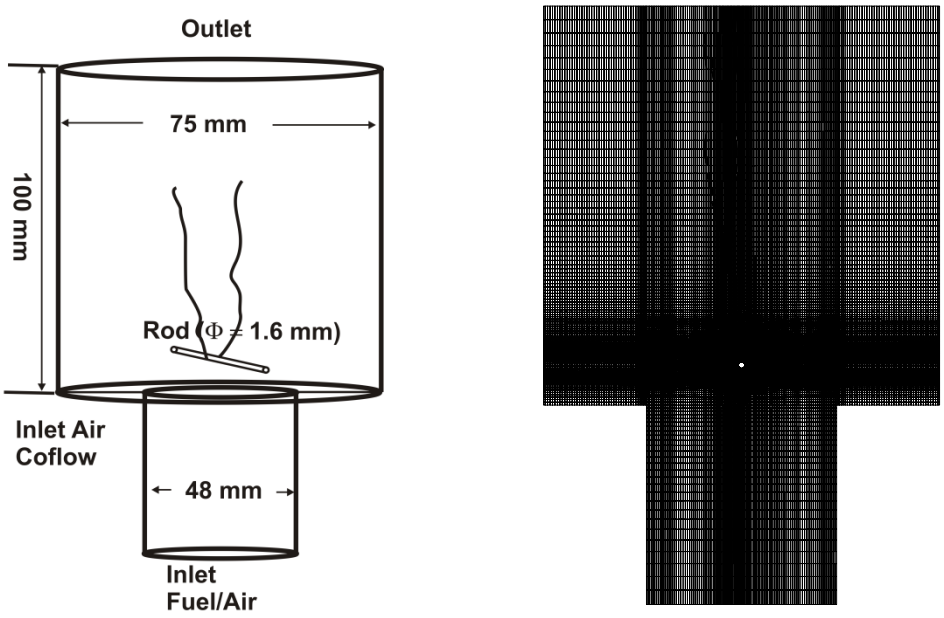

Figure 1: Numerical geometry (right) and grid (left) of rod stabilized flames

The non-reacting and reacting flow simulations are carried out using numerical domain which has height and diameter of 100 and 75 mm, respectively. The inflow

velocity was generated by the bottom section of the experimental set up. This section has the inlet diameter of 76 mm with turbulence grid in the middle and the outlet diameter is 48 mm. Bottom section has 1 million tetrahedra grids, and the inlet profile is taken from 50 mm below the outlet. The upper simulation section is meshed with hexahedra grids of approximately 3 million grid points. The cell size and refinement have been carried out according to the position, the domain is splited into 4 sections with 30 blocks. The maximum expansion ratio of 1.1 is used for creating the structured grids.

The inlet profile from this simulation is used for the other non reacting and reacting flow cases. The cold flow simulations are carried out at 300 K, atmoshperic pressure for the mass flow rate of 9 and 25 kg/hr. The Reynolds number of the flow for 9 and 25 kg/hr are 3770 and 10250 based on the inlet diameter and 124 and 345 on rod diameter. The inlet turbulence intensity is considered as 10 %, it is the similar value of the experimentally observed value. Air at 300 K and 1 bar is considered for non reacting case and the fuel-air mixture is considered for reacting case at equivalence ratio of 0.8 and 0.87. Coflow air of velocity 0.5 m/s is used into the bottom of the domain. The reaction flow simulation is carried out by initialising a small region above the rod as ignition source.

Inlet is assigned with velocity inlet boundary conditions, Outlet is prescribed with zero normal gradient, outer cylinder is assigned as symmetry boundary condition. Walls are considered to be non moving, adiabatic and smooth. For time and space discretization, implicit second order and bounded second order schemes are employed with convergence criteria and time steps of 1e-06 and 5e-05, respectively, for CFL of 0.5. RANS simulations are carried out for each conditions and the converged solution is used as an initial guess for unsteady flow and flame simulations. Each LES case is run for ten flow-through times of which the first half is used to get a quasi periodic flow and the second half for statistical averaging of output data.

4 RESULTS AND DISCUSSIONS

4.1 Non-reacting flow comparison

RANS and LES turbulence models are employed for simulating non-reacting flows in the current flow past a cylindrical rod case. Inlet inflow is separately simulated in a section of 50 mm distance away from the exit of the turbulence grid. This generated flow velocity profile is given as inlet velocity profile for all simulations whose results are presented here. In steady RANS simulations, there is no oscillating flow observed, while in LES, a peak of oscillation frequencies (f) of 110 Hz and 360 Hz, for 9 and 25 kg/hr (with the corresponding Strouhal number (St=fd/U) are 0.154 and 0.18), respectively, are observed (Fig.2). These two LES quantities f and St (shown in table 1) are in good agreement with the previously published data [3]. The quantities f and St are calculated by collecting axial velocity data at 10 mm above the rod and analyzed by using Fast Fourier Transform in MATLAB program. Mean flow numerical data comparisons at position 8 mm below the rod are in good agreement with the experiments (Fig.3).

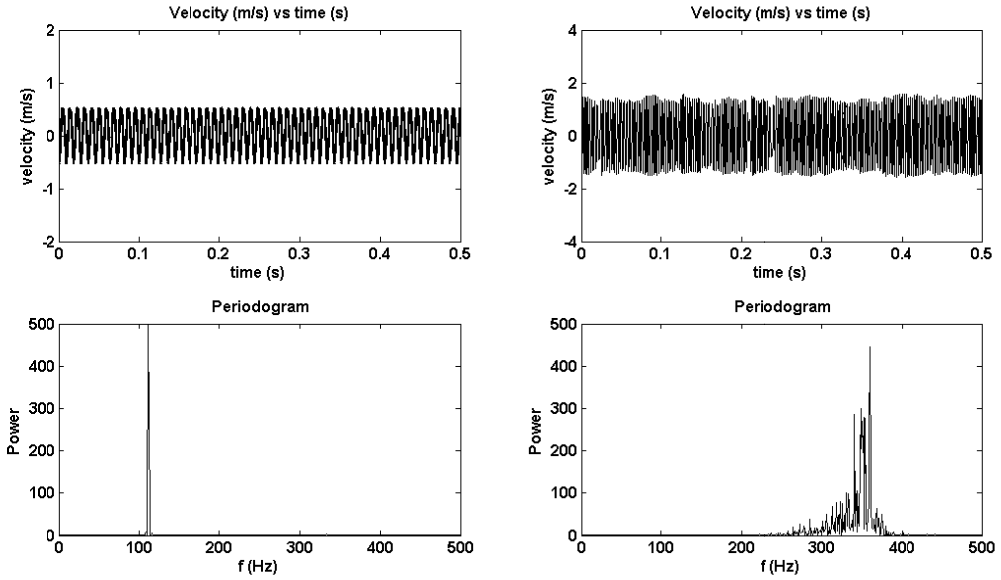

Figure 2: Lateral velocity vs. time (top) and power vs. vortex shedding frequency f (bottom) for 9 (left) and 25 kg/hr (right) for the non-reacting flow with the SM model, taken 10 mm distance from the rod

Mass flow rate m (kg/hr)	Velocity U (m/s)	Re (rod)	Re (geometry)	LES (SM)			RANS (RNG)
				f (Hz)	St	C_d	C_d
9	1.15	124	3660	110	0.154	1.38	1.47
25	3.2	345	10250	360	0.18	1.17	1.12

Table 1: Comparison of shedding frequency (f), the Strouhal number (St) and drag coefficient (C_d)

The flow behavior is visualized by axial velocity contours shown in Figures 4, 5 and 6. RANS steady simulations with RNG k-ε model does not show any sign of vortex shedding behind the rod (Fig.4). Figure 5 shows the alternating vortex shedding behind the rod and the variation of side jet interaction with the co-flow. The same figure shows a narrow wake region with smaller area of shedding at low flow rate condition when compared to high flow rates with broader wake and larger area of shedding. Similar findings are found from LES, shown in Fig.6.

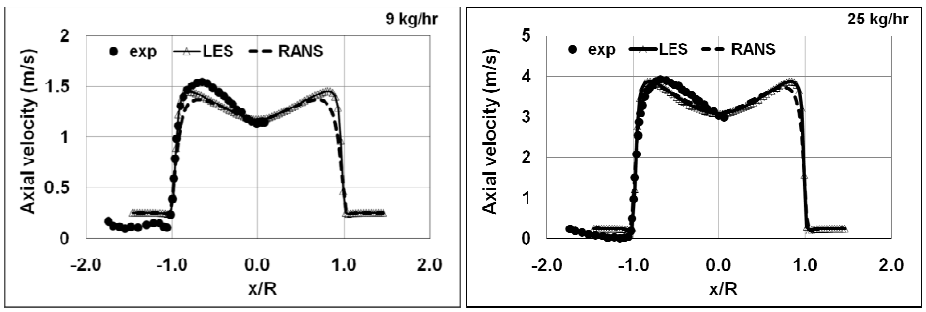

Figure 3: Axial flow velocity comparison for the experimental and simulation results for 9 and 25 kg/hr measure 2 mm above the exit of the inlet

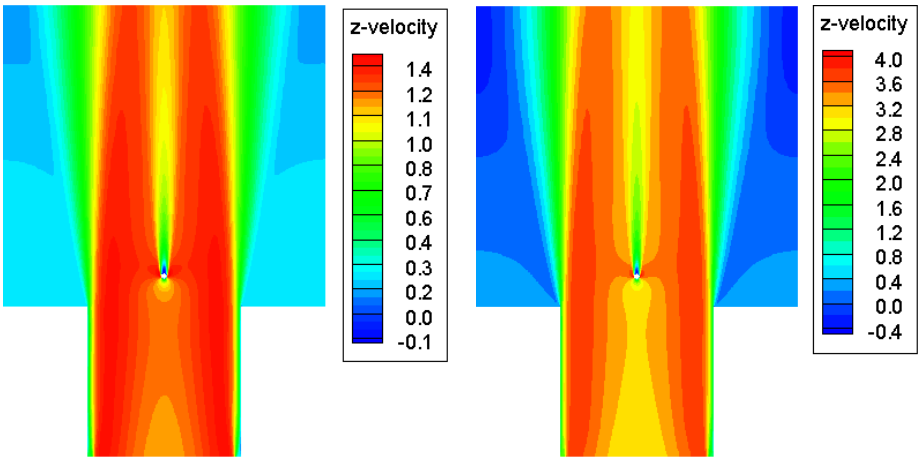

Figure 4: Contours of simulated axial flow velocity comparison for 9 (left) and 25kg/hr (right) with RNG k-ε model and 2.7 million grid points

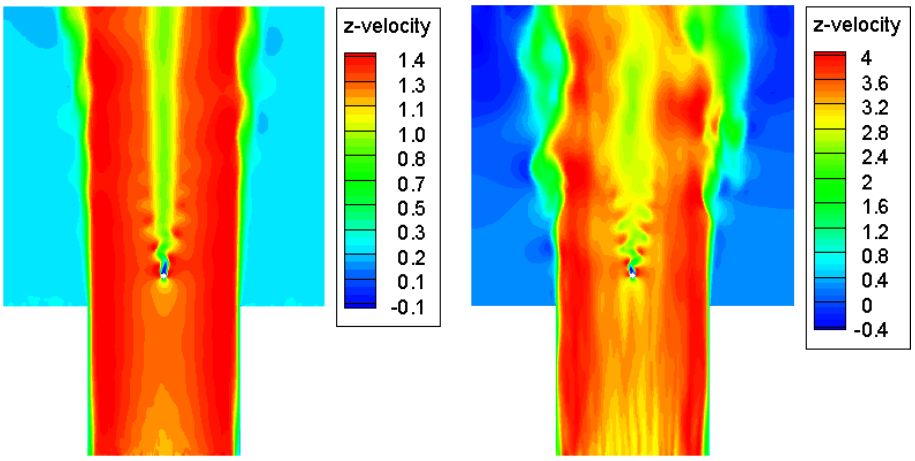

Figure 5: Contours of simulated instantaneous axial flow velocity for 9 (left) and 25 kg/hr (right) with the Smagorinsky subgrid scale model for 2.7 million grid points

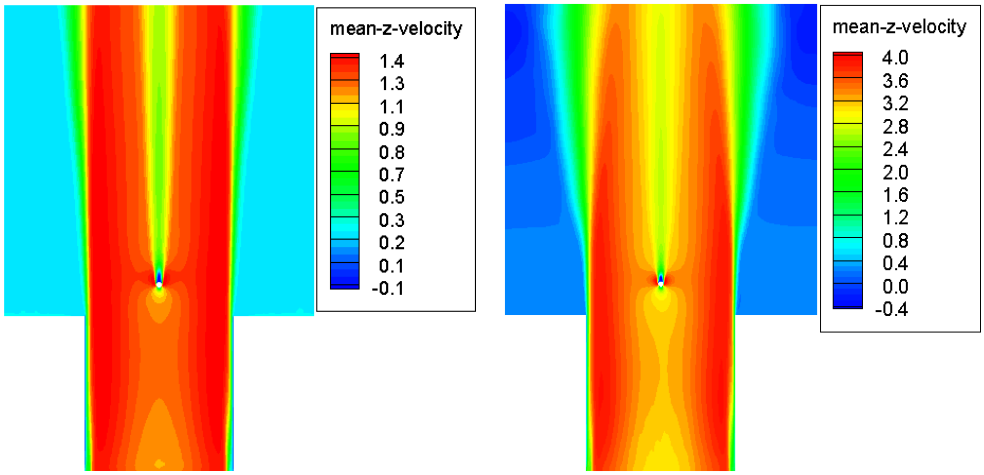

Figure 6: Contours of simulated averaged mean axial velocity for 9 (left) and 25 kg/hr (right) with the Smagorinsky subgrid scale model and 2.7 million grid points

The drag force coefficent ($C_d = F_d/(1/\rho v^2 A)$) is calculated based on inlet boundary conditions and properties and the values are listed in Table 1. For RANS turbulence model, the predicted C_d does not vary after attaining a constant but different value for each case. In LES, the drag coefficient is associllating between 1.0 and 1.5 for both conditions. These data are shown in Fig. 7. Quantitative differences in C_d between RANS and LES predictions is well below 5 percentage.

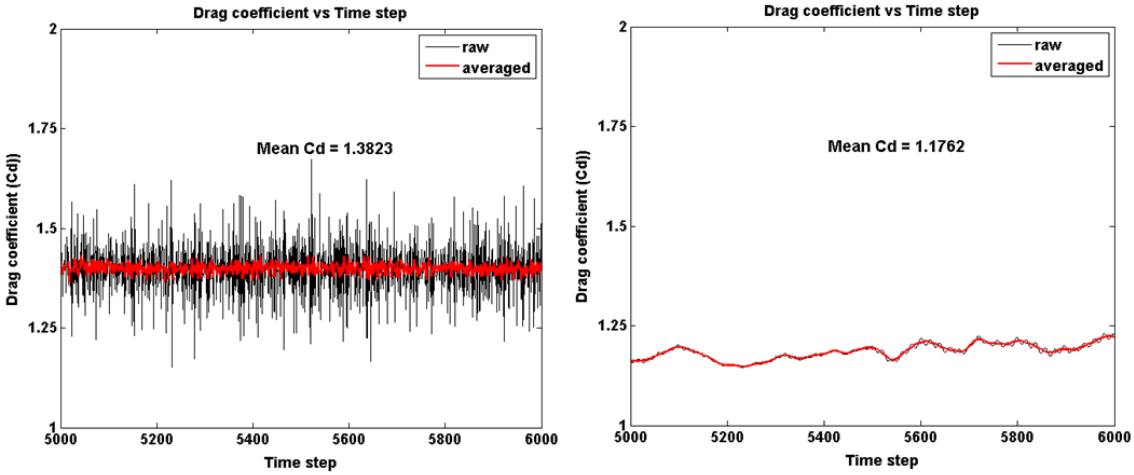

Figure 7: Non reacting flow drag coefficient (C_d) predictions for 9 and 25 kg/hr of air with the Smagorinsky subgrid scale model

4.2 Reacting flow comparison

The flame simulations are carried out with the AFSW and the TFC reaction closures for variation of mass flow rate and equivalence ratio. For both RANS and LES turbulence models, the reaction closures are implemented in the solver as User Defined Functions (UDF) [8]. The effect of co-flow air is also included into the reaction simulation by solving addition passive scalar equation. For comparison, the half flame angle (θ) is determined from the experimental progress variable contours, and it is angle between c = 0.5 and the vertical flow-axis by considering rod as starting position.

Figure 8 shows the simulated flame contours for methane fuel. Both reaction models capture the experimental flame shape and angle (34°) at 9 kg/hr conditions. However, the flame brush predicted by the AFSW model shows good agreement with experimental trend of increasing brush thickness along the flow direction. At 25 kg/hr, the TFC model over predicts the flame angle by 6° and the AFSW shows a small deviation of 1° with experiments (shown in Table 2). At higher equivalence ratio from 0.80 to 0.87, the flame angle and the brush are well predicted by the AFSW model.

For a propane case, the AFSW model prediction matches very well with the experimental flame angle, while the TFC model shows slight deviation. This is explained with diffusivity effects of individual species in the fuel-air mixture. The methane-air mixture has the Lewis number (Le=mass diffusivity(α)/heat diffusivity(D)) close to unity. For the propane-air mixture, the Lewis number is 1.62, i.e. the heat diffusivity is higher than the mass diffusivity. This effect is explicitly included in the AFSW reaction model. This study demonstrates the importance of the Lewis number effects in reaction modelling.

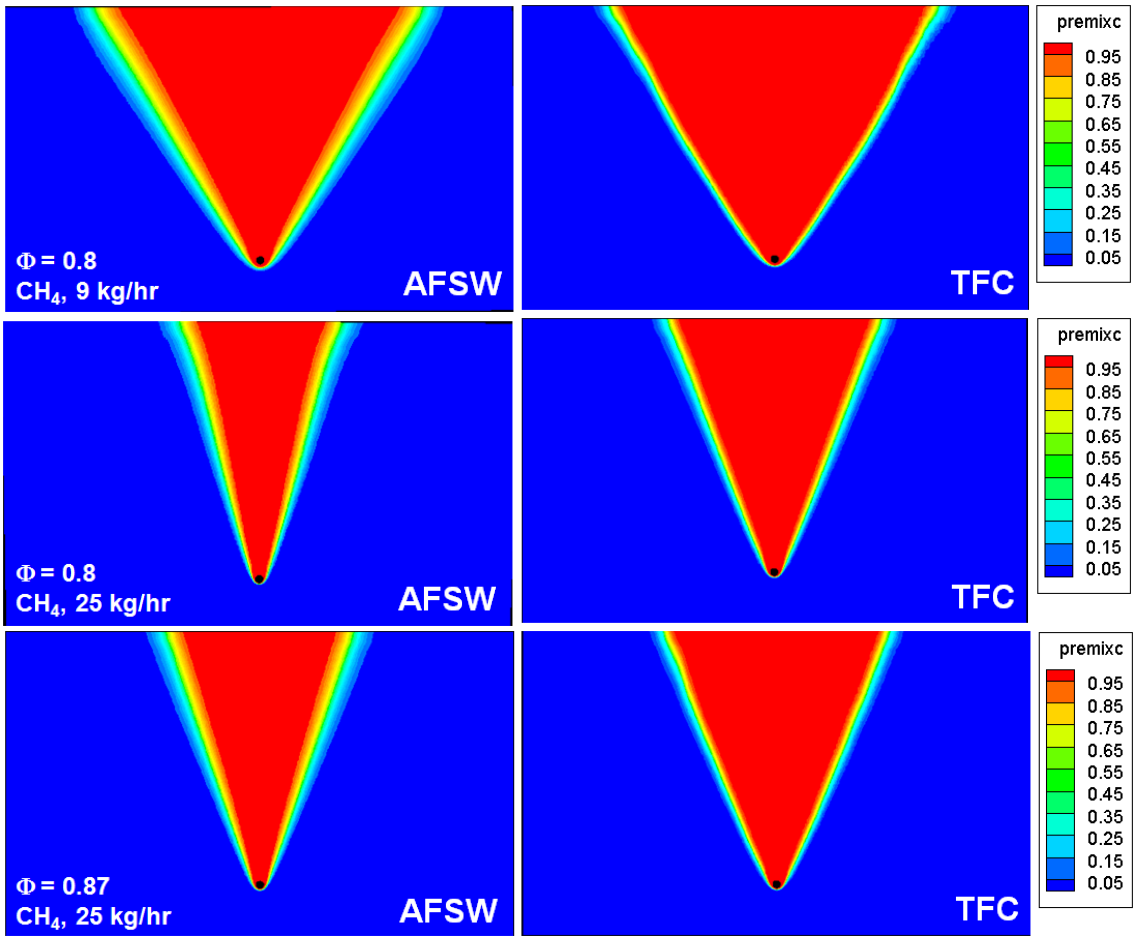

Figure 8: Compared contours of predicted reaction progress variables of the AFSW and the TFC reaction models at equivalence ratio (Φ) of 0.8, 0.87 and 9 & 25 kg/hr for methane (CH_4)-air mixture and RNG k-ε model, where, c= 0 (blue) unburned and c=1 (red) burned

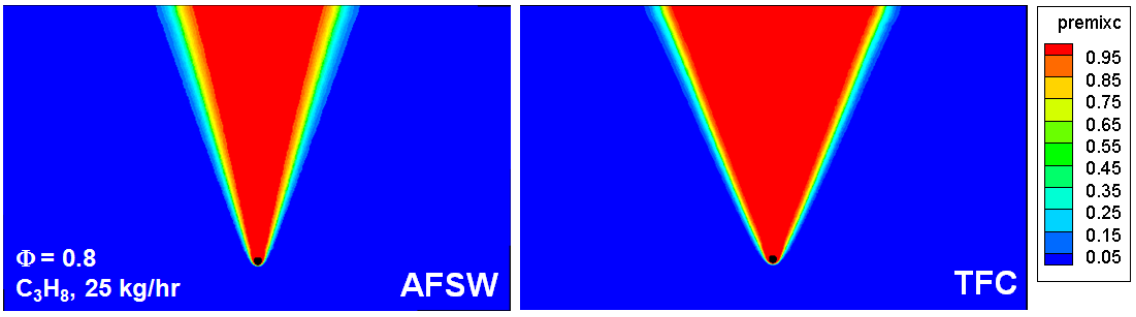

Figure 9: Compared contours of predicted reaction progress variables using the AFSW and the TFC reaction models at equivalence ratio (Φ) of 0.8 and 25 kg/hr for propane (C_3H_8)-air mixture and RNG k-ε model where, c= 0 (blue) unburned and c=1 (red) burned

Fuel	Methane			Propane
m (kg/hr)	9	25		25
Equivalence ratio (Φ)	0.8	0.8	0.87	0.8
Exp (Θ)	33	17	22	17
AFSW (Θ)	34	18	21	18
TFC (Θ)	34	23	24	24.5

Table 2: Flame half angle (θ) comparison with experimental observations

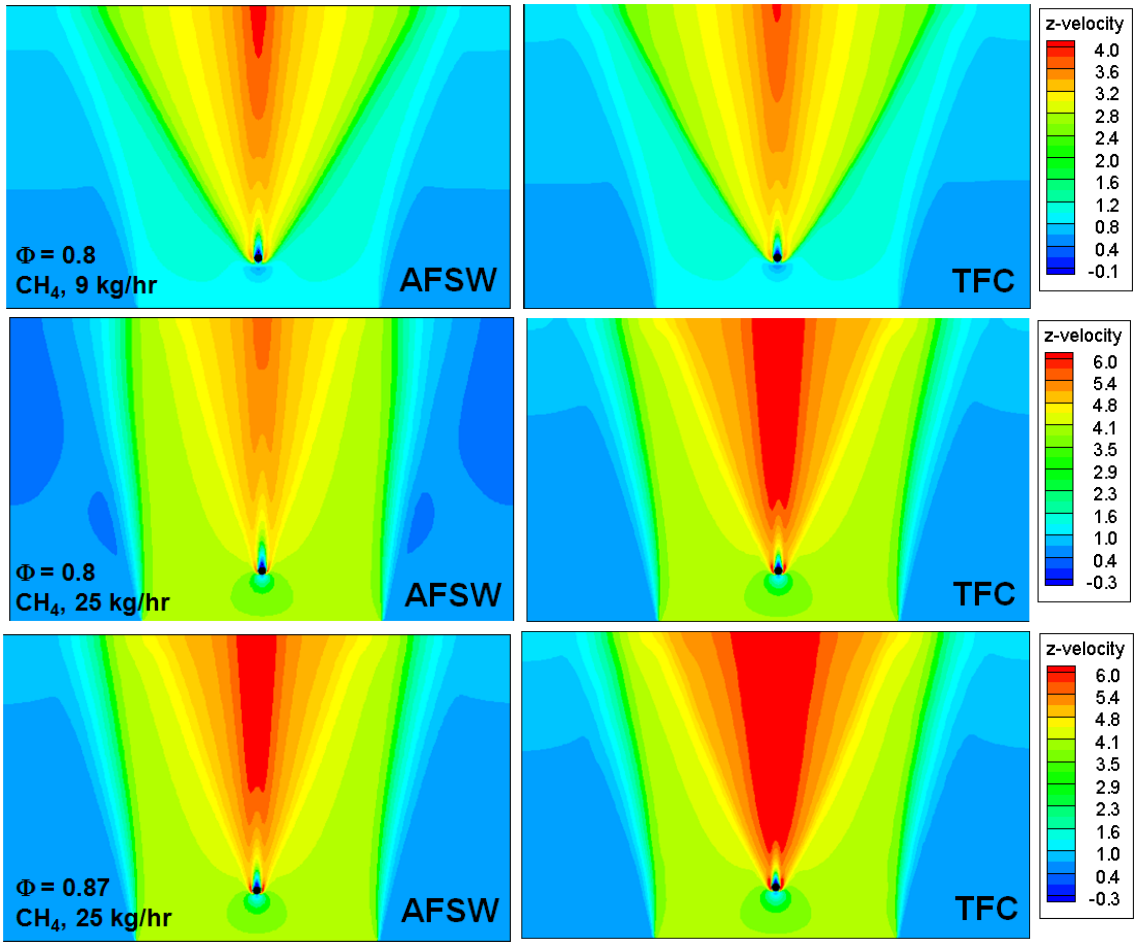

Figure 10: Compared contours of predicted axial velocity using the AFSW and the TFC reaction models at equivalence ratio (Φ) of 0.8, 0.87 and 9, 25 kg/hr for methane (CH_4)-air mixture and RNG k-ε model

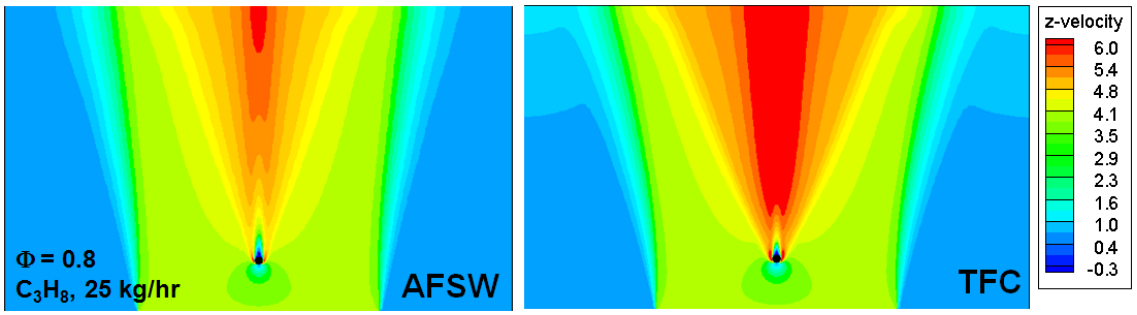

Figure 11: Compared contours of predicted axial velocity using the AFSW and the TFC reaction models at equivalence ratio (Φ) of 0.8 and 25 kg/hr for propane (C_3H_8)-air mixture and RNG k-ε model

Fuel	Methane			Propane
m (kg/hr)	9	25		25
Equivalence ratio (Φ)	0.8	0.8	0.87	0.8
AFSW (C_d)	2.22	1.21	1.23	1.21
TFC (C_d)	2.36	1.34	1.37	1.36

Table 3: Drag coefficient (C_d) comparison between two reaction models in RANS

Comparison of axial velocity contours are made between the two reaction models, shown in Figures 10 and 11. It can be noted here that corresponding experimental reacting data could not be compared due to unavailability of literature data. These contours show that the velocity in the wake region reaches up to 4 m/s, which is almost three times higher than at 9 kg/hr. Axial flow velocity predicted by the TFC show a broader wake region than by the AFSW model at 25 kg/hr and the ratio between velocity reaches up to 1.5.

The drag coefficient (C_d) is calculated for reacting flows for RANS turbulence models and the values are presented in Table 3. The C_d value increases up to 50 % for low mass rate flow and up to only 20 % for higher flow rate. The results also show that the drag coefficient is almost independent of the equivalence ratio and fuel type. Thus, it can be concluded that C_d in reacting flow is mainly dependent on the inlet mass flow rate.

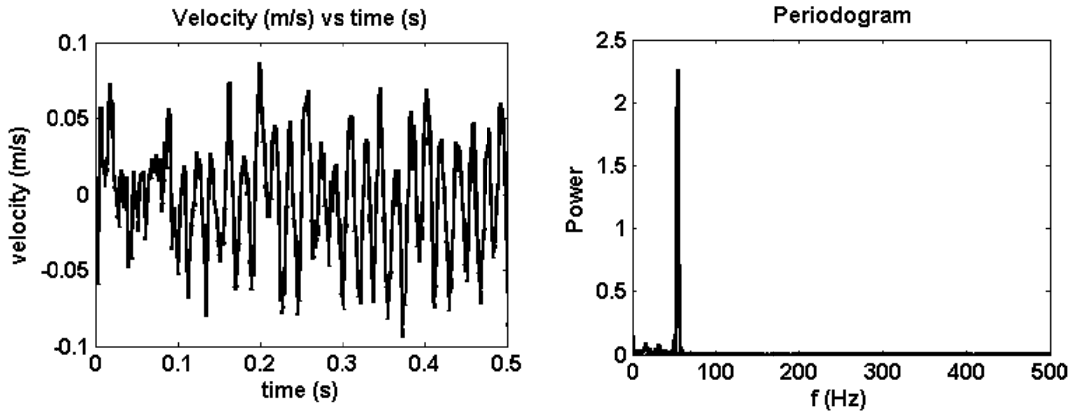

Figure 12: Lateral velocity vs. time (top) and power vs. vortex shedding frequency f (bottom) for 25 kg/hr, Φ=0.8 for the reacting flow with the SM model, taken 10 mm distance from the rod

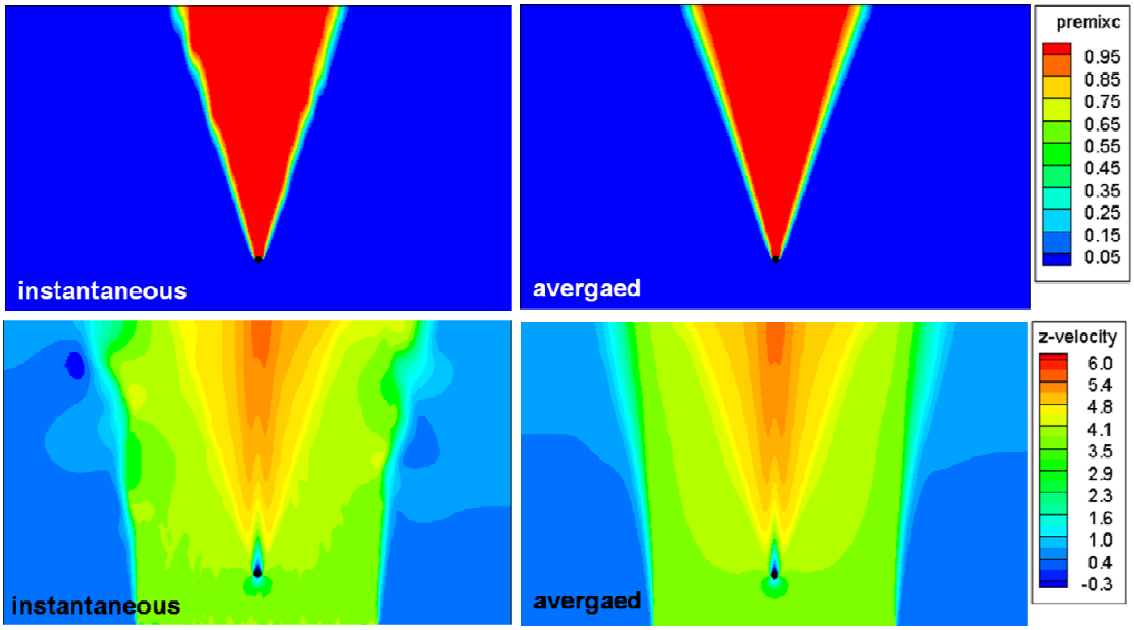

Figure 13: Compared contours of predicted progress variable (top) and axial velocity (bottom) using the AFSW reaction model at equivalence ratio (Φ) of 0.8, 25 kg/hr for methane (CH_4)-air mixture with LES – the Smagorinsky subgrid scale model

Combustion-LES is carried out for the 25 kg/hr, equivalence ratio of 0.8. The lateral mean flow velocity data collected 10 mm above the rod shows a large difference in fluctuation between non-reacting and reacting flows at the same conditions, are presented in Figure 12. This flow quantity is almost dampened due to combustion heat release. The observed frequency under this condition is 53 Hz and the calculated Strouhal number is 0.0265. Fig. 13 shows instantaneous and averaged V-flame in terms of reaction progress variable (top). These contours show that the flame brush thickness increases in the axial flow direction (bottom), and it is relatively thinner compared to thinner than that from RANS.

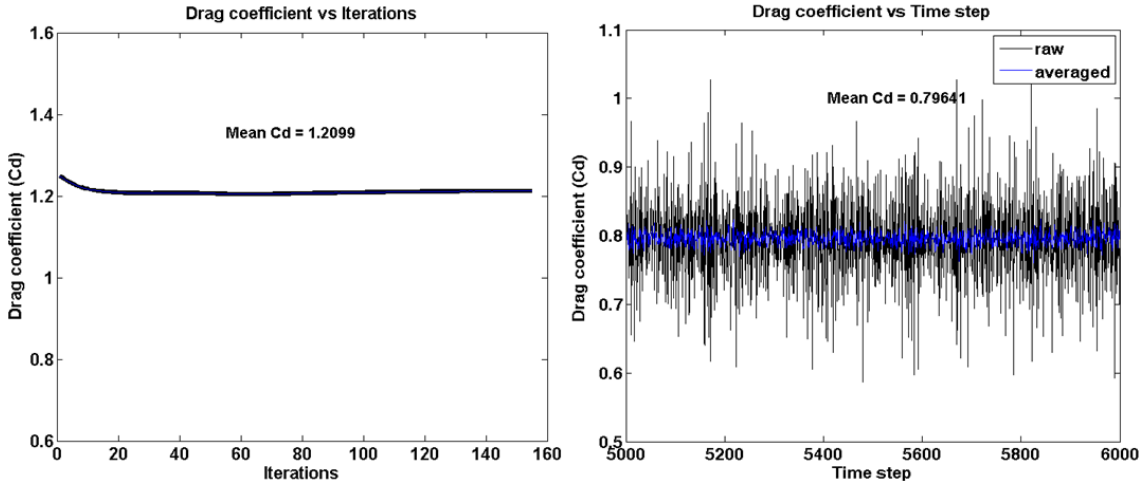

Figure 14: Reacting flow drag coefficient (C_d) with RANS and LES turbulence model at 25 kg/hr, equivalence ratio of 0.8

The drag coefficient (C_d) at 25 kg/hr and equivalence ratio of 0.8 from LES is 0.8, which is 33 % lower than RANS value, as shown in Fig. 14. This difference is attributed to predicted differences in flame attachment position close to the rod. In RANS simulations, the flame is anchored in the bottom portion of the rod, whereas in LES it is on the top side. DNS studies by Bell at al. [2] showed that the flame is attached to the bottom of the rod and propagate in the flow direction which forms a V-shape reaction zone, which is the trend of RANS predictions. In contrary Bell et al. noted that DNS and experiment deviate in flame stabilization position. More detailed LES studies are required for improved characterization of flame morphology.

5 CONCLUSION

Numerical simulations of laboratory scale rod (1.6 mm) stabilized V-shaped flame were carried out using an Algebraic Flame Surface Wrinkling (AFSW) reaction model. The Two fuels methane and propane at equivalence ratios 0.8 and 0.87 at two mass flow rates (9 & 25 kg/hr) were used. Comparative studies were carried out against experimental findings of Pfadler et al. with those obtained from the Turbulent Flame speed Closure (TFC) model. The predicted results showed that the flame angle predicted by the AFSW model is in good agreement with experiment. The TFC model show slight deviation overprediction for propane mixture and higher mass flow rate.

For non-reacting flow, RNG k-ε model showed no vortex shedding, whilst LES predicted shedding frequencies of 110 and 360 Hz and Strouhal number on 0.154 and 0.18 at 9 kg/hr and 25 kg/hr, respectively. Overall, non-reacting mean flow quantities were in good agreement with experiments. For reacting flow, at 25 kg/hr and

equivalence ratio of 0.8, the shedding frequency of 53 Hz and Strouhal number of 0.0265 was found in LES. The drag force analysis revealed that the drag coefficient increases for the reacting flow by 10-50 % as compared to drag coefficient of non-reacting flows. It was noticed that drag coefficient showed significant deviation with inlet flow rate, while it was found to be less sensitive to fuel type and fuel composition. LES produced reverse trends; the drag force coefficient decreased for reacting flow, due to shift in flame anchoring position. Concerning the force analysis on reacting flows, more LES studies are required.

REFERENCES

1. Muppala, S. P. R., Aluri, N. K., Dinkelacker, F., and Leipertz, A., *Development of an algebraic reaction rate closure for the numerical calculation of turbulent premixed methane, ethylene and propane/air flames for pressures up to 1.0 MPa.* Combustion and Flame, 2005. 140: p. 257-266.
2. Bell, J. B., Day, M. S., Shepherd, I. G., Johnson, M. R., Cheng, R. K., Grcar, J. F., Beckner, V. E., and Lijewski, M. J., *Numerical simulation of a laboratory-scale turbulent V-flame.* PNAS, 2005. 102(29): p. 10006-10011.
3. Zdrakovich, M. M., *Flow around circular cylinder (vol 2: Applications)*. First edition ed. 2003, Great Britain: Oxford University Press.
4. Baranyi, L., Szabo, S., Bollo, B., and Bordas, R., *Analysis of low Reynolds number flow around a heated circular cylinder.* Journal of Mechanical Science and Technology, 2009. 23: p. 1829-1834.
5. Veynante, D. and Vervisch, L., *Turbulent Combustion Modeling.* Progress in Energy and Combustion Science, 2002. 28: p. 193-266.
6. Poinsot , T. and Veynante, D., *Theoretical and numerical combustion*. Second edition ed. 2005, Philadelphia: Edwards.
7. Sagaut, P., *Large eddy simulation of incompressible flows*. Third edition ed. 2006, Heidelberg: Springer.
8. Fluent, *ANSYS Incorporated*, in *Lebanon, NH, USA*. 2006.
9. Flohr, P. and Pitsch, H. *A turbulent flame speed closure model for LES of industrial burner flows*. in *Center for Turbulence Research, Proceedings of the Summer Program 2000*. 2000. Stanford.
10. Zimont, V. L. and Lipatnikov, A. N., *A numerical model of premixed turbulent combustion of gases.* Chem. Phys. Reports, 1995. 14(7): p. 993-1025.
11. Pfadler, S., Kerl, J., Beyrau, F., Leipertz, A., Sadiki, A., Scheuerlein, J., and Dinkelacker, F., *Direct evaluation of the subgrid scale scalar flux in turbulent premixed flames with conditioned dual-plane stereo PIV*. Proceedings of the Combustion Institute, 2009. 32.